Limited Set of Amino Acid Residues in a Class Ia Aminoacyl-tRNA Synthetase Is Crucial for tRNA Binding†

Renaud Geslain,‡ Gilbert Bey,§ Jean Cavarelli,§ and Gilbert Eriani*,‡

UPR 9002 SMBMR du CNRS, Institut de Biologie Moléculaire et Cellulaire, 15, rue René Descartes, 67084 Strasbourg, France, and UMR7104 Laboratoire de Biologie et Génomique Structurales, Institut de Génétique et de Biologie Moléculaire et Cellulaire, CNRS, INSERM, ULP, 1, rue Laurent Fries, BP163, 67004 Illkirch, France

Received September 3, 2003; Revised Manuscript Received October 16, 2003

ABSTRACT: The aim of this work was to characterize crucial amino acids for the aminoacylation of $tRNA^{Arg}$ by yeast arginyl-tRNA synthetase. Alanine mutagenesis was used to probe all the side chain mediated interactions that occur between $tRNA^{Arg2}_{ICG}$ and ArgRS. The effects of the substitutions were analyzed in vivo in an ArgRS-knockout strain and in vitro by measuring the aminoacylation efficiencies for two distinct $tRNA^{Arg}$ isoacceptors. Nine mutants that generate lethal phenotypes were identified, suggesting that only a limited set of side chain mediated interactions is essential for tRNA recognition. The majority of the lethal mutants was mapped to the anticodon binding domain of ArgRS, a helix bundle that is characteristic for class Ia synthetases. The alanine mutations induce drastic decreases in the tRNA charging rates, which is correlated with a loss in affinity in the catalytic site for ATP. One of those lethal mutations corresponds to an Arg residue that is strictly conserved in all class Ia synthetases. In the known crystallographic structures of complexes of tRNAs and class Ia synthetases, this invariant Arg residue stabilizes the idiosyncratic conformation of the anticodon loop. This paper also highlights the crucial role of the tRNA and enzyme plasticity upon binding. Divalent ions are also shown to contribute to the induced fit process as they may stabilize the local tRNA-enzyme interface. Furthermore, one lethal phenotype can be reverted in the presence of high Mg^{2+} concentrations. In contrast with the bacterial system, in yeast arginyl-tRNA synthetase, no lethal mutation has been found in the ArgRS specific domain recognizing the Dhu-loop of the $tRNA^{Arg}$. Mutations in this domain have no effects on $tRNA^{Arg}$ aminoacylation, thus confirming that *Saccharomyces cerevisiae* and other fungi belong to a distinct class of ArgRS.

Aminoacyl-tRNA synthetases (ARS)[1] link tRNAs with their cognate amino acid generally through a reversible two-step reaction in which the first step consists of the activation of the amino acid by ATP to produce aminoacyl-adenylate with release of pyrophosphate. In the second step, the activated compound is transferred onto the 3′ end of the cognate tRNA molecule. Each of the ARSs discriminates against chemically and structurally very similar substrates with a very high specificity.

Aminoacyl-tRNA synthetases have been classified into two classes, on the basis of two scaffolds of the active site core characterized by conserved amino acid residues (*1*, *2*). Class I ARSs are built around a canonical dinucleotide binding fold (Rossmann fold), whereas class II ARSs share a mixed β-sheet partly closed by helices. Aminoacyl-tRNA synthetases constitute one of the best textbook examples of multidomain proteins including a large diversity of insertion and terminal functional modules appended to one of the two class-specific active-site architectures. Diversity is also found at the level of the quaternary structure where at least five types of oligomeric structure are found: α, $\alpha 2$, $\alpha\beta$, $\alpha 2\beta 2$, and $\alpha 4$. Monomeric ARSs, which all belong to class I, display some peculiar behavior. Among them, three of the canonical class I ARSs (ArgRS, GlnRS, and GluRS) and the recently discovered class I type LysRS are unable to catalyze the activation of the amino acid without the presence of their cognate tRNA. This requirement is supposed to establish the specific recognition of the substrates. Three other monomers (IleRS, LeuRS, and ValRS) have acquired additional domains to edit the wrong amino acid they may activate and charge.

Arginyl-tRNA synthetase (ArgRS) is one of the monomeric enzymes that needs cognate tRNA to activate arginine. The question as to why ArgRS requires its tRNA to activate arginine has been addressed by X-ray crystallography. Four crystal structures of the yeast *Saccharomyces cerevisae* ArgRS (yArgRS) have been solved, three of them corresponding to complexes of yArgRS and one of its cognate tRNAs, the second major $tRNA^{Arg}$ isoacceptor in yeast ($tRNA^{Arg2}_{ICG}$) (*3*, *4*). The highest resolution (2.2 Å) has been obtained with a ternary complex of ArgRS and $tRNA^{Arg}$ in the presence of the L-arginine substrate. On the basis of these

† This work was funded by the Centre National de la Recherche Scientifique and grants from Union Européenne (4ème Program des Biotechnologies "Design of RNA Domains, Substrates or Inhibitors of tRNA Recognizing Proteins").

* To whom correspondence should be addressed. Phone: 33 3.88.41.70.42. Fax: 33 3.88.60.22.18. E-mail: G.Eriani@ibmc.u-strasbg.fr.

‡ Institut de Biologie Moléculaire et Cellulaire.

§ Institut de Génétique et de Biologie Moléculaire et Cellulaire.

[1] Abbreviations: ARS, aminoacyl-tRNA synthetase; *RRS1*, ArgRS gene; 5-FOA, 5-fluoroorotic acid; Dhu, dihydrouridine; ACBS, anticodon binding site; 3-D, three-dimensional.

10.1021/bi035581u CCC: $25.00
Published on Web 11/21/2003

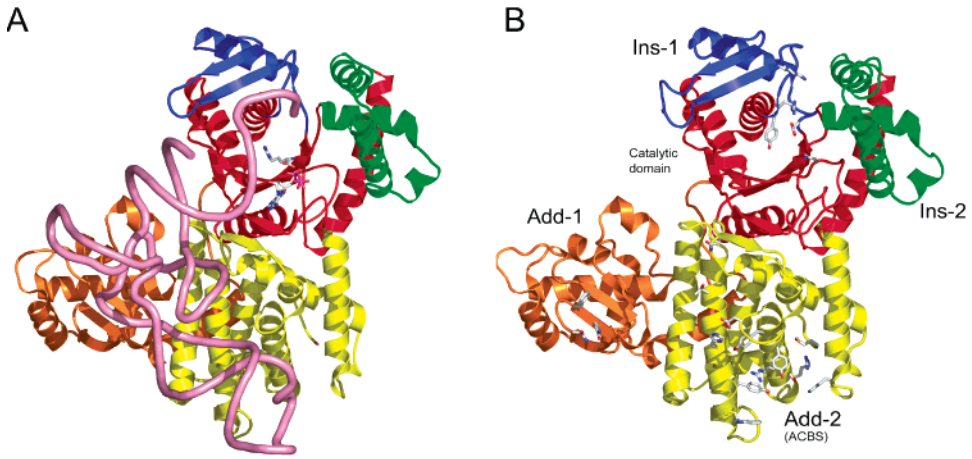

FIGURE 1: Overall structure of arginyl-tRNA synthetase in complex with $tRNA^{Arg2}_{ICG}$. (A) Overview of one monomer of yArgRS interacting with $tRNA^{Arg2}_{ICG}$ (Figures 1 and 2 were drawn with PyMol (*47*)). The $tRNA^{Arg2}_{ICG}$ backbone is drawn with its phosphate chain traced with a thick pink line. The substrate L-arginine is shown into the active site, as well as the putative position of the ATP molecule obtained from structural superimposition with the ternary complex GlnRS:$tRNA^{Gln}$:ATP (*48*). (B) Overview of one monomer of yArgRS. The 18 mutated side chains of the protein are shown. Three of them (N106, F109, and Q111) are located in the N-terminal domain (Add1). Two other residues (N153 and Y347) are located in the catalytic core, and the 13 other residues are located in the C-terminal domain (Add2 or ACBS). Add-1 or ArgRS specific domain is formed by residues 1−143; the catalytic domain comprises residues 144−194, 267−293, 346−410; Ins-1 is made of residues 195−266 and Ins-2 of residues 294−345; Add-2 or ACBS is composed of residues 411−607.

structures, the yeast ArgRS can be schematically divided into five domains (Figure 1): the catalytic domain and two additional (Add1 and Add2) and two insertion domains (Ins1 and Ins2). Add1 and Add2, two nucleic acid binding modules, are attached, respectively, at the N- and C-terminal sides of the active site. The active site of ArgRS, which forms the scaffold of the Rossmann fold, is composed of two halves assembled from three peptides. Domain Ins1 is inserted into the first half of the catalytic core, while domain Ins2 links the two halves of the Rossmann fold.

Add1 and Add2 of yArgRS cooperate for $tRNA^{Arg}$ recognition, and the contact area can be schematically divided into three different parts: (i) the first zone of interaction involves Add2 and the tRNA anticodon loop, (ii) the second zone involves the Dhu-stem and Dhu-loop of the tRNA and Add1 of the protein, and (iii) the third zone of contact involves the end of the acceptor stem and the terminal CCA interacting with the catalytic center of the protein (Figure 1).

Add1, the ArgRS specific domain, is the most characteristic domain of ArgRS and is missing in other class I ARS structures. Moreover, no other domain has been found at a similar spatial position in all other class I ARSs. This is correlated to the main function of domain Add1, the specific recognition of the Dhu-loop of the $tRNA^{Arg}$ (*4*). The core of domain Add1 exhibits similar topology with several other RNA binding proteins including a module of the ribosome recycling factor protein. Add2, an α-helical domain, is the most widespread domain in ARSs after the catalytic domain characteristic of each class since a similar module has been found in mainly all other class Ia ARSs (CysRS, IleRS, LeuRS, MetRS, and ValRS). Add2 corresponds to the anticodon binding site (ACBS) of those enzymes.

The enzyme and the $tRNA^{Arg}$ form an extensive interface, and two schemes of interactions are found. Interactions with the three important recognition signals of the $tRNA^{Arg}$ (the nucleotides of the anticodon loop, the Dhu20 of the Dhu-loop, and the 3′-terminal CCA) are mainly direct protein−RNA interactions, while the binding of the amino acid acceptor stem is mainly achieved by water mediated interactions. These different schemes of interactions may be correlated with the high variability in the sequences of the amino acid acceptor ends of the four $tRNA^{Arg}$ isoacceptors in yeast *S. cerevisiae*. One may therefore hypothesize that the water mediated interactions confer a high adaptability to the interface while providing the required specificity and affinity.

More than giving a detailed picture of the interactions between the substrates and the enzyme, those crystal structures reveal that several key residues of the active site play multiple roles in the catalytic pathway. Comparison of those structures revealed that while ArgRS requires its cognate tRNA for the first step of the aminoacylation reaction, the presence of $tRNA^{Arg}$ is not a prerequisite for L-arginine binding. Moreover, using a molecular switch based on two different conformations of a phylogenetically invariant tyrosine, it has been shown that L-arginine binding is a prerequisite that triggers the correct positioning of the CCA end of the tRNA. The structural data have also shown that the binding of $tRNA^{Arg}$ produces conformational changes of the ATP binding cleft and builds up the functional ATP binding pocket. Communications between the different modules of ArgRS that contribute to the efficiency and specificity of the arginylation reaction have also been revealed.

In parallel to this structural work, using random mutagenesis followed by a genetic screening in yeast, we have isolated 26 mutations that inactivate *S. cerevisiae* ArgRS (*5*). Eighteen mutated residues were found in the catalytic site around the arginine binding pocket. Eight others were found into the C-terminal domain of the enzyme (Add2). They act on the catalytic site through a distal effect by strongly impairing the rates of tRNA charging and arginine activation.

In the present work, all the ArgRS residues that are located at a hydrogen-bonding distance of the $tRNA^{Arg}$ molecule and involved in nonwater mediated RNA−protein interactions have been mutated into alanine residues. ArgRS mutants were first tested in vivo for the complementation of a yeast

knockout strain deprived of ArgRS. The mutated proteins were then overexpressed in *Escherichia coli* and were analyzed in vitro for the kinetic parameters with two different $tRNA^{Arg}$ isoacceptors. In addition, the in vivo steady-state level of charging of the four $tRNA^{Arg}$ isoacceptors was studied by Northern blot under acidic conditions.

This paper focuses on the analysis of the tRNA binding site of yeast ArgRS and reveals the existence of a conserved set of functional amino acid residues shared by the other class Ia synthetases (CysRS, IleRS, LeuRS, MetRS, and ValRS). It then reveals several clues on the evolution process of the $tRNA^{Arg}$ recognition in a group of lower eukaryotes comprising several fungi.

EXPERIMENTAL PROCEDURES

Strains, Plasmids, and Yeast Strain Manipulations. E. coli TB1 (F^- ara Δ(lac-proAB) hsdR (rk^- mk^+) rpsL(Str^r) [ϕ80, dlac Δ (lacZ)M15] was used as a recipient for cloning procedures. The haploid *S. cerevisiae* YAL4 (n rrs1::HIS3 ura3−52 lys2−801^{am} trp1-Δ63 his3-Δ200 leu2-Δ1 ade2-Δ450 ade3-Δ1483 pAL4 [Ura^+, $Ade3^+$, $RRS1^+$]) was used to assay the mutant phenotypes. This strain carries a knockout of the ArgRS gene (*RRS1*) and is maintained by a plasmidic copy of the native gene (*5*). The bacterial and yeast strains were grown and transformed according to standard procedures.

Plasmid pTrc99B was used to express the mutants of yeast ArgRS in *E. coli* (*5*). Plasmid pRS314-*RRS1* contained the native ArgRS gene and *TRP1* marker. The uracil single strand template was used to generate the ArgRS variants by site-directed mutagenesis (*6*). To assay the mutant phenotypes, the shuffle protocol previously described was used (*5*). The YAL4 strain was transformed with the mutated pRS314-*RRS1* and plated on minimal medium supplemented with adenine (limiting concentration of 2 μg mL^{-1}), histidine (20 μg mL^{-1}), uracil (20 μg mL^{-1}), lysine (20 μg mL^{-1}), and leucine (60 μg mL^{-1}). After a 72 h incubation at 30 °C, the Trp^+ colonies were isolated and checked for their colored phenotypes (red nonsectoring colonies: sect−, or white/red sectoring colonies: sect+). Then they were screened for 5-FOA resistance (5-FOA was from Toronto Research Chemicals, Canada). The Trp^+ red (sect−) and 5-FOA^S colonies were unable to lose their rescuing pAL4 plasmid; they contained an inactive ArgRS gene on the pRS314 plasmid. For the shuffle assay with increasing Mg^{2+} concentrations, minimal medium with adenine, histidine, uracil, lysine, and leucine (see above for concentrations) was supplemented with increasing concentrations of $MgCl_2$: 1, 5, 20, 50, 100, 250, and 500 mM. The white/sectoring phenotype was observed as above.

Overexpression of the Different ArgRS. The mutated ArgRS genes were cloned into the bacterial expression vector pTrc99B-*RRS1* by replacing the 1.9 kbp DNA fragment EcoRI-XhoI of the native *RRS1*. The recipient strain TB1 was grown to an OD_{700} of 0.5 and then induced by adding IPTG to a final concentration of 0.5 mM. After 12 h of induction, the cells were harvested by centrifugation and washed with TE buffer (10 mM Tris-HCl (pH 8), 1 mM EDTA). Enzyme extraction and purification to homogeneity was essentially performed according to the protocol established for AspRS (*7*), except that the ArgRS protein was eluted from the hydroxyapatite column with 150 mM potassium phosphate buffer (pH 7.5).

Measurement of Kinetic Parameters. The aminoacylation mixture contained 100 mM HEPES-NaOH (pH 7.5), 30 mM KCl, 0.1 mg/mL bovine serum albumin, 5 mM glutathione, 5 mM ATP, 50 μM L-[^{14}C] arginine (25−350 Ci/mol), L-[^{14}C] arginine (Amersham Biosciences, UK), 5−15 mM $MgCl_2$, and 10 μM pure $tRNA^{Arg}$ or 200 μM unfractionated tRNA. The reaction was initiated by the addition of enzyme and followed at 37 °C. At varying time intervals (usually 1 min), aliquots of 20 μL were spotted onto Whatman 3 MM disks and TCA precipitated, the and radioactivity was measured by liquid scintillation. For ATP and $tRNA^{Arg}$ K_M measurements, the substrate concentrations were varied from 0.25 to 2 times the K_M value. We used yeast total tRNA from Boehringer Mannheim (Batch 12375221−66) to measure the K_M for ATP and a free excess of 2 mM $MgCl_2$. To measure the K_M for $tRNA^{Arg}$, we used a concentration of 5 mM ATP and 5 or 12 mM $MgCl_2$.

For the ATP−PPi exchange reaction, the mixture contained 100 mM HEPES-NaOH (pH 7.5), 10 mM $MgCl_2$, 2 mM [^{32}P]PPi (1−2 cpm/pmol), 5 μM $tRNA^{Arg2}_{ICG}$ (purified according to ref *4*), 2 mM ATP, 15 mM arginine, and 10 mM KF. The reaction was started by enzyme addition, and after various incubation times at 37 °C, 20 μL aliquots were measured for [^{32}P]ATP formation. For arginine K_M measurements, the arginine concentrations were varied from 0.25 to 2 times the K_M value.

RNA Analysis. Crude yeast RNA was prepared by phenol extraction under acidic conditions according to ref *8*. A total of 30 μg of RNA was separated under acidic conditions by denaturing PAGE (10%) and transferred on Hybond-XL membrane (Amersham Pharmacia Biotech). Membranes were hybridized at 60 °C with one of the $tRNA^{Arg}$ probes, a 5S probe (control for RNA content), and a $tRNA^{Leu}_{UAA}$ probe (control for the acidic extraction procedure). The probes were $tRNA^{Arg1}_{CCU}$ (5′TGGCGTTCCGTACGGGACTC), $tRNA^{Arg2}_{ICG}$ (5′TGGCTTCCCCGCCAGGACTT), $tRNA^{Arg3}_{UCU}$ (5′GAACCCATAATCTT CTGATTAGAAG), $tRNA^{Arg4}_{CCG}$ (5′CTCGAACCCGGATCACAGCC), 5S (5′ACCCAC TACACTACTCGGTCAGGCTCTTAC), and $tRNA^{Leu}_{UAA}$ (5′GGATGCGAGGTTCGAA CTCGCGCGG) (oligonucleotides were from Genset, France). The quantification of signals was performed with a Fuji Bioimager Bas2000.

RESULTS

On the basis of the crystal structure of yeast ArgRS in complex with $tRNA^{Arg2}_{ICG}$, we selected 18 residues of ArgRS that interact by their side chains with the tRNA at distances less than 3.5 Å (Figure 1) (*4*). Three of them (N106, F109, and Q111) are located in the N-terminal domain (Add1). Two other residues (N153 and Y347) are located in the catalytic core and interact with Ade76 of the tRNA. The 13 other residues are located in the C-terminal domain (Add2 or ACBS); they are mainly binding the concave face of the L-shape of the tRNA from the elbow region to the anticodon-loop of the tRNA (Table 1). Among the 18 selected residues, five are strictly conserved in all ArgRS sequences; these are N153, Y347, Y491, R495, and M607. Five other residues (F109, Y488, S498, R501, and Y565) are highly conserved in all ArgRS sequences. Six other residues show limited

Table 1: Growth Phenotypes of the TRNA^{Arg} Binding Site Mutants of ArgRS[a]

protein residue	phenotype of the alanine mutation in the ArgRS-knockout strain	tRNA nucleotide
Asn106 (Oδ1)	viable	Dhu20 (O2, N3)
Phe109 (stacking)	viable	Dhu20 (stacking)
Gln111 (Nε2)	viable	Dhu20 (O4)
Asn153 (Oδ)	lethal	Ade76 (O2′)
Tyr347 (N, stacking)	lethal	Ade76 (O1P, stacking)
Lys439 (Nζ)	viable	Gua36 (O1P)
Asn469 (Nδ2,Oδ1)	lethal	Ade14, Cyt13, 6 (O2P, O3′)
Asp484 (N,Oδ2)	viable	Gua23, 24 (O2′,O4′)
Tyr488 (OH)	lethal	Cyt40 (O1P)
Tyr491 (OH)	lethal	Ade38, Gua36 (O1P, O2′)
Arg495 (NH1, NH2)	lethal	Gua36, Ade37, Cyt39 (O2′,O1P)
Ser498 (Oγ)	viable	Gua36 (O2P, N7)
Arg501 (NH2)	viable	Gua36 (O6)
Thr552 (Oγ1)	viable	Ade14 (O2′)
His559 (Nε2, Nδ1)	lethal	Gua23, Cyt40, Tyr488 (O2′,O2P,OH)
Tyr565 (O, OH)	viable	Cyt35, Gua36 (N4, O2P)
Trp569 (stacking)	lethal	Ino34, Cyt35 (stacking)
Met607 (N, OT1, OT2)	viable/lethal[b]	Gua36, Ade38 (O6N1N6)

[a] Atom groups of both tRNA and synthetase molecules are indicated as well as the phenotypes of the corresponding alanine mutants observed in the yeast ArgRS-knockout strain. The three-code letter has been used for amino acids and nucleotides. [b] Two mutants of residue M607 were constructed: MA607 was viable, and M607stop was lethal.

Table 2: Aminoacylation Properties for the Two Major tRNA^{Arg} Isoacceptors[a]

		charge of tRNA$^{Arg2}_{ICG}$		charge of tRNA$^{Arg3}_{UCU}$	
	Mg^{2+}(mM)	K_M(μM)	k_{cat}(s^{-1})	K_M(μM)	k_{cat}(s^{-1})
native	3.5			0.1	5
	5	0.15	8		
NA106	3.5			0.02	4
	5	0.1	8		
FA109	3.5			0.08	6
	5	0.25	7		
QA111	3.5			0.06	7
	5	0.07	10		
NA153	3.5			0.06	0.009
	5	0.4	0.01		
YA347	3.5			nm	<0.0005
	5	nm	<0.0005		
NA469	3.5			0.65	0.0006
	5	0.4	0.001		
	12	0.3	0.0003	0.10	0.002
YA488	3.5			0.07	0.09
	5	0.2	3		
	12	0.07	2	0.08	*0.8*
YA491	3.5			0.13	0.007
	5	0.2	0.16		
	12	0.1	0.17	0.05	*0.1*
RA495	3.5			0.5	0.001
	5	0.3	0.005		
	12	0.2	*0.2*	0.2	*0.05*
HA559	3.5			0.4	0.04
	5	0.5	3		
	12	0.2	3	0.1	2
YA 565	3.5			0.2	0.4
	5	0.15	0.5		
	12	0.2	*3*	0.05	*3*
WA569	3.5			0.2	0.1
	5	0.2	0.8		
	12	0.2	*4*	0.1	*2*
MA607	3.5			0.06	0.35
	5	0.1	5		
	12	0.05	2.6	0.03	*2*
M607stop	3.5			0.15	0.02
	5	0.07	0.25		
	12	0.1	0.5	0.05	*0.1*

[a] Measurements were done at three different Mg^{2+} concentrations. Italicized numbers indicate significant increases of activity on magnesium concentration variation. The data in this table are the average values with a variation of <25% from three independent determinations.

conservation among ArgRS sequences (K439, N469, D484, T552, H559, and W569), whereas two residues located in the N-terminal domain (N106 and Q111) are only conserved in class-A ArgRS sequences (see below).

The 18 residues were mutated into alanine residues, and the mutated genes were tested for their ability to rescue the *RRS1*-disrupted strain YAL4. In addition, we also constructed a deletion mutation of the last residue (M607) of ArgRS. Among these 19 mutations, nine induced lethal phenotypes. For these nine lethal mutants and five viable mutants, the proteins were expressed in *E. coli* and purified, and their catalytic properties were analyzed.

Nine Mutations Induce Lethality in the Yeast Cells. Nine mutations are lethal in the yeast strain disrupted for the ArgRS gene (Table 1). These mutations can be arranged into two groups according to the 3-D structure.

A first group includes three mutations (NA153, YA347, and NA469); N153 and Y347 are located in the active site of the protein and are involved in the catalytic reaction, and N469 belongs to the tRNA-anchoring platform that interacts with the concave face of the tRNA.

The second group contains five Ala mutations located in the C-terminal domain (YA488, YA491, RA495, YA559, and WA569) and in addition, a deletion of the last residue of the protein (M607stop). M607 is a quasi-invariant residue that stabilizes the distorted anticodon loop conformation by its main chain atoms and stabilizes Y491 by its side chain atoms. Therefore, two mutants were generated to test the two types of interactions: a substitution (MA607) to remove the side chain and a deletion (M607stop) to remove both side chain and main chain. The in vivo assay has shown that only the deletion mutant was unable to rescue the knockout strain, whereas the alanine substitution was viable. This demonstrates that M607−main chain interactions that occur with nucleotides 36 and 38 have an essential function in vivo (see Table 1).

Kinetic analyses have been performed on these purified mutant proteins. The k_{cat} and K_M values for ATP, arginine, and two tRNA isoacceptors (tRNA$^{Arg2}_{ICG}$ and tRNA$^{Arg3}_{UCU}$) have been measured. Our work also includes analyses of the effect of the Mg^{2+} concentration and misacylation properties of tRNA^{Asp}. Data are summarized in Tables 2 and 3.

All nine lethal mutants exhibit large decreases in both ATP−PPi-exchange and tRNA-charging reactions. Remarkably, for the five mutants in the C-terminal domain, these effects were coupled to decreases in ATP binding strength. Only slight changes in tRNA affinity and no effect on arginine binding were observed, except for the mutant of residue N153 that is involved in both tRNA and arginine binding.

The five lethal mutants of the C-terminal domain require an unusually high Mg^{2+} concentration to reach their highest catalytic rate. The optimal Mg^{2+}/ATP ratio for the native ArgRS is 1, while for these mutants the ratio was increased up to 2.5 (Figure 3). This was observed with tRNA$^{Arg2}_{ICG}$ and more often with tRNA$^{Arg3}_{UCU}$, which seemed to be more

Table 3: Catalytic Properties of the Mutated ArgRS Proteins[a]

	aminoacylation reaction		ATP−PPi-exchange reaction	
	K_M ATP (mM)	$k_{cat}(s^{-1})$	K_M arginine (μM)	$k_{cat}(s^{-1})$
native	0.3	1	5	15
NA106	0.3	1	nd[b]	nd
FA109	0.3	2	4	16
QA111	0.3	1.5	nd	nd
NA153	2	0.4	50	0.1
YA347	3	0.05	nm[c]	<0.005
NA469	1.4	0.002	nm	0.005
YA488	0.7	0.3	5	4
YA491	9	0.2	6	0.7
RA495	3	0.03	6	0.9
HA559	0.7	0.4	3	3
YA565	0.6	1	4	9
WA569	0.8	0.3	2	2
MA607	1.6	0.4	5	3
M607stop	5	0.05	5	0.3

[a] The data in this table are the average values with a variation of <25% from three independent determinations. [b] nd, not determined. [c] nm, nonmeasurable.

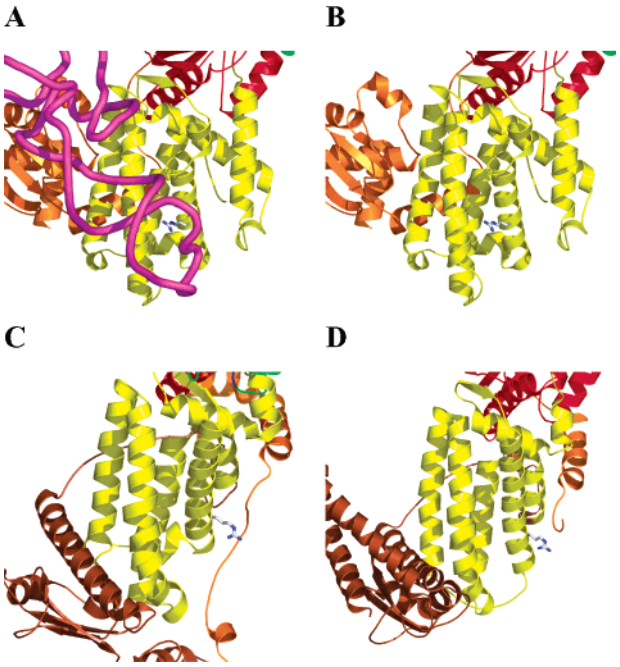

FIGURE 2: View of helix bundle domain (shown in yellow) of three class Ia aminoacyl-tRNA synthetases illustrating the structural position of the highly conserved arginine. This domain is found in all six class Ia ARSs (ArgRS, CysRS, IleRS, LeuRS, MetRS, and ValRS). Only three of them, for which the structures are known in the presence of the cognate tRNA, are displayed here. Panels A and B correspond to yArgRS (PDB code 1F7U); panel C corresponds to *S. aureus* IleRS (PDB code 1FFY); and panel D corresponds to *T. thermophilus* ValRS (PDB code 1IVS). For clarity of the figures, the conformation of the cognate tRNA is only shown for yArgRS in panel A. Despite a common fold, the helices of the ACBS domain have idiosyncratic deformations. In the three known structures of class Ia ARS:tRNA complexes, the conserved arginine residue (R495 in yArgRS, R653 in IleRS, and R587 in ValRS) is involved in the stabilization of the idiosyncratic conformation of the cognate tRNA.

sensitive to the divalent ion concentration. In contrast, such excesses of Mg^{2+} inhibited both active site mutants (NA153 and YA347), the mutant NA469 located in the β-hairpin (data not shown), as well as the native ArgRS.

Moreover, as wild type yeast ArgRS spontaneously catalyzes the misacylation of the heterologous $tRNA^{Asp}$ (*9*),

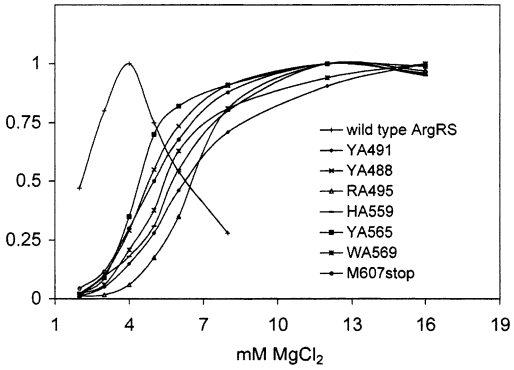

FIGURE 3: Mg^{2+} dependence of the aminoacylation of $tRNA^{Arg3}_{UCG}$ by yeast ArgRS. For clarity, all the relative activities have been normalized to one.

the misacylation properties of all ArgRS mutants were also analyzed. Two mutants (YA491 and RA495) of the ACBS have exhibited a significant increase of the misacylation ratio of the heterologous $tRNA^{Asp}$. The increase was about 10-fold as compared to the level of the native ArgRS (data not shown).

Mutations in the N-Terminal Domain Have No Effects on tRNA Aminoacylation. Fungi as *S. cerevisiae* differ from bacteria and most of the other organisms by the absence of the quasi-invariant nucleotide Ade20 that is the major identity element of $tRNA^{Arg}$ (*10*, *11*). To analyze the function of the corresponding Dhu20 and Cyt20 found in *S. cerevisiae* $tRNA^{Arg}$, we have constructed mutants of the ArgRS residues that recognize these residues. The 3-D structure of ArgRS in complex with $tRNA^{Arg2}_{ICG}$ shows that N106, F109, and Q111 bind Dhu20 in a specific way and suggests that the same residues could also recognize the nucleotide Cyt20 in $tRNA^{Arg3}_{UCU}$ by a flip of their side chains (*4*). The mutants were analyzed for their in vivo and in vitro properties, including the aminoacylation of the four different $tRNA^{Arg}$ isoacceptors.

In a first step, the mutants were tested in vivo in the ArgRS-knockout strain. All the mutants were able to rescue the disrupted strain, demonstrating an absence of dramatic effect on the mutant properties (Table 1). In addition to the three single mutants, we built two double mutants (NA106 + FA109) and (FA109 + QA111) to investigate the combined effect of the individual mutations. Both double mutants were also able to sustain the cell growth of the disrupted strain (data not shown). Altogether, these data show that the interactions that occur between the protein and the Dhu-loop of $tRNA^{Arg}$ do not play an essential role in vivo.

The absence of an in vivo effect contrasts with the structural data and the phylogenetic analyses that predict the presence of a conserved binding mechanism (J. Cavarelli and G. Eriani, unpublished data). Therefore, the in vitro catalytic parameters of the three single mutants NA106, FA109, and QA111 were analyzed to detect partial inactivation. However, we could not observe any significant change on the steady-state kinetic parameters and on the K_M for ATP, arginine, $tRNA^{Arg2}_{ICG}$, and $tRNA^{Arg3}_{UCU}$. Thus, both in vitro and in vivo results are in good agreement.

To verify the steady-state levels of aminoacylation of the four $tRNA^{Arg}$ isoacceptors in vivo, we performed Northern blot analyses under acidic conditions (*8*). Figure 4 shows the hybridization pattern observed with $tRNA^{Arg2}_{ICG}$, one of

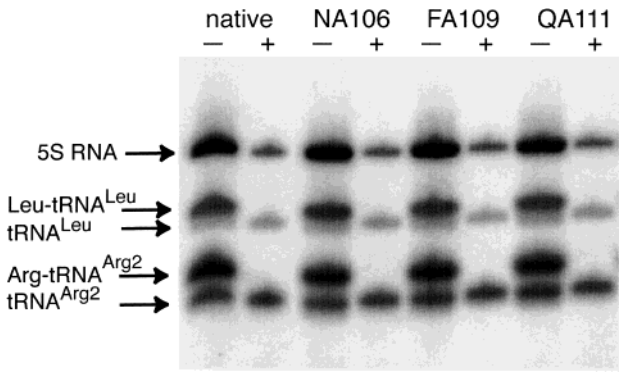

FIGURE 4: Northern blot analysis of tRNA extracts electrophoresed on a 6.5% polyacrylamide gel containing 8 M urea (pH 5.0), at 4 °C. Total RNA was extracted under acidic conditions, separated, and transferred to Hybond membrane. The blot was probed with a mixture of ^{32}P-labeled oligonucleotides complementary to 5S RNA (control for RNA content), to tRNA^{Leu} (control for the acidic extraction procedure), and to tRNA$^{Arg2}_{ICG}$. The aminoacylation level is given by comparison of the deacylated samples (lanes +, obtained at pH 9.0) and the acid samples (lanes −). 30 μg of total RNA was loaded in the − lanes (acid samples) and 10 μg in the + lanes (deacylated samples).

the major tRNA^{Arg}. Quantification of the signals shows that the Arg-tRNA^{Arg} levels are similar when comparing the native and mutant samples. In vivo, the level of aminoacylated tRNA$^{Arg2}_{ICG}$ reaches 71%, a value similar to those measured for the other isoacceptors: 68% for tRNA$^{Arg1}_{CCU}$, 74% for tRNA$^{Arg3}_{UCU}$, and 59% for tRNA$^{Arg4}_{CCG}$ (data not shown). These results definitely confirm that the single mutations NA106, FA109, and QA111 have no effect on the aminoacylation of any tRNA^{Arg} isoacceptor. These data collectively demonstrate that despite a conserved framework of tRNA recognition, the recognition of residue 20 in the yeast does not follow the canonical rules of tRNA^{Arg} identity and differs from most living organisms.

DISCUSSION

Binding of the Dhu-Arm but Not Dhu-Loop Is Important for Aminoacylation by Yeast ArgRS. In many tRNAs, the major identity elements are found in the anticodon triplet and at the discriminator base. However, some systems have evolved to select their identity elements outside of the anticodon. In tRNA^{Arg}, the highly conserved residue Ade20 of the Dhu-loop is one of the major identity elements of the bacterial system (*10*−*12*). However, fungi like *S. cerevisiae* or *Schizosaccharomyces pombe*, *Neurospora crassa*, and some mitochondrial tRNA^{Arg} contain Cyt or Dhu instead of the canonical Ade20. In tRNA^{Arg} from *S. cerevisiae*, it was shown that this residue is not an identity element but rather an antideterminant for noncognate enzymes such as *E. coli* ArgRS. Accordingly, when mutated into Ade20, the yeast tRNA becomes a good substrate for the *E. coli* enzyme (*13*). More recently, it was shown that yeast cells can grow with tRNA$^{Arg4}_{CCG}$ carrying the UA20 or UG20 mutations (*14*). The only detectable effect was on the steady-state levels of the aminoacylated tRNA, which were decreased by a factor of 3.5 in vivo. Therefore, unlike in the *E. coli* tRNA^{Arg}-ArgRS system where residue 20 (Ade) is a major identity element, in yeast this position is of limited consequence (*14*).

However, the crystal structure of the yArgRS:tRNA^{Arg} complex reveals a specific recognition mode between ArgRS and the Dhu-loop of the tRNA, which was not expected from the biochemical data obtained for *S. cerevisiae* ArgRS. The yArgRS:tRNA^{Arg} complex is the first structural example in which the Dhu-loop plays a crucial role for tRNA selectivity. The ArgRS specific domain of yArgRS recognizes the Dhu-loop of the tRNA^{Arg} and interacts specifically with nucleotide Dhu20. Moreover, the yArgRS:tRNA^{Arg} complex together with the analysis of the ArgRS sequences suggests two schemes of recognition for the nucleotide in position 20 of the tRNA^{Arg}. Phylogenetically, very conserved amino acids create a partition of ArgRS sequences into two classes, each class using a different scheme of recognition of nucleotide 20 using the same structural platform. The first class (class-A ArgRS) contains ArgRS from yeast and very few other organisms, while the second one (class-B ArgRS) includes all other organisms. Class-A ArgRSs recognize nucleotide at position 20 in tRNA^{Arg} (Dhu20 in yeast tRNA^{Arg2}) by mainly three invariant residues: N106, F109, and Q111. F109, a highly conserved residue in all ArgRS sequences, is involved in a stacking type interaction with Dhu20. Residues N106 and Q111 are only conserved within class-A ArgRS. Class-B ArgRSs recognize an invariant Ade20 in tRNA^{Arg} with an asparagine residue located in position 111 (yArgRS numbering). Position 106 in class-B ArgRSs (yArgRS numbering) is occupied by a tiny residue to accommodate the adenosine ring. Class-B ArgRS is therefore characterized by an adenosine−asparagine interaction. On the basis of the yArgRS:tRNA^{Arg} complex, which corresponds to the class-A enzyme, a model of Ade20 recognition by the canonical ArgRS (class-B) has been proposed. This model has been validated by site-directed mutagenesis of *Thermus thermophilus* ArgRS (*15*).

In this paper, we have shown that single and double mutants that cumulate the loss of interactions have no consequence on the in vivo and in vitro parameters. Moreover, no effect was observed on the growth phenotype of the ArgRS-knockout strain. The in vitro aminoacylation parameters of these mutants were unchanged for the two major tRNA^{Arg} isoacceptors. Moreover, we could see no difference in the in vivo steady-state levels of the aminoacylated forms of the four tRNA^{Arg} isoacceptors as shown by Northern blot analyses under acidic conditions. Altogether, the results suggest that the three residues have not the crucial importance suggested by the structural data. This contrasts remarkably with the *T. thermophilus* ArgRS, where Ala mutations of the F109- and Q111-equivalent residues (Y77 and N79, respectively) induce a drastic inactivation of the ArgRS (*15*). This discrepancy between the results of both systems can be explained by the fact that fungi like *S. cerevisiae* bind other nucleotides than Ade20. Dhu20 or Cyt20 are frequently found in these organisms (*16*). Thus, we suggest that during evolution, fungi have gradually reduced the importance of the interaction with nucleotide 20 of tRNA^{Arg}. Alternatively, we cannot exclude that these interactions are maintained for the negative role they could play against noncognate tRNAs. However, such loss of function would lead to lethal dominant mutants unable to grow, a phenotype that we did not observe.

A significant loss in binding energy should obviously result from the loss of the canonical Dhu-loop interactions. Therefore, we examined the results of the mutational analysis to find some interactions able to counterbalance this loss. In

the neighboring region, we found that a nonconserved residue (N469) generates a strong effect when replaced by an alanine residue. The NA469 mutant was unable to rescue the ArgRS-knockout strain and displayed a very low activity and one of the highest K_M values for $tRNA^{Arg2}_{ICG}$ and $tRNA^{Arg3}_{UCU}$ charging. N469 is localized in the β-hairpin formed by strands S13 and S14 on which the Dhu-loop side of the tRNA seats and interacts (*4*). In the crystal structures of the tRNA-bound ArgRS, N469 mainly interacts with the phosphate of nucleotide Ade14. It therefore appears that N469 stabilizes the unusual conformation of the Dhu-loop resulting from the presence of an additional non-Watson−Crick base pair between residues Ade14 and Ade21. Moreover, a shift of the β-hairpin is observed upon tRNA binding, suggesting that in addition to the Dhu-loop stabilization, this interaction might participate in the induced fit mechanism that may transmit the anticodon binding signal to the catalytic site. Residue N469 is not conserved in the different ArgRS sequences; a small residue (A, S, or T) is often found in this position in other known sequences. However, an asparagine residue is only found in a minority of organisms including the fungi *S. cerevisiae*, *S. pombe*, and *N. crassa*. Thus, in these organisms, N469 is certainly involved in the structural features that compensate in Class-A ArgRS for the lack of catalytically productive recognition of the canonical identity element A20.

However, it should be pointed out that this loss of binding energy caused by the lack of catalytically productive interactions with the Dhu-loop in Class-A ArgRS may be also compensated by supplementary interactions involving main chain atoms of the protein. A complete understanding of those effects requires at least a structure of a complex containing a Class-B ArgRS and its cognate $tRNA^{Arg}$ in addition to the structures already known; unfortunately, such a structure is not yet available.

Six Residues of ACBS Are Essential for tRNA Aminoacylation. A previous study has shown that nucleotides Cyt35, Gua36, or Uri36 of the anticodon loop are the major identity elements of yeast $tRNA^{Arg3}_{UCU}$ (*17*). In addition, it was shown that a Gua38 was not tolerated. The crystal structure of the complex with $tRNA^{Arg2}_{ICG}$ confirms that Cyt35, Gua36, and Ade38 are recognized in a base specific manner by side chain and by main chain interactions with the ArgRS C-terminal domain. The anticodon loop adopts a highly distorted conformation that seems to be entirely dedicated to the binding of the strongest identity element C35 (*4*).

In the present paper, we identified six residues that displayed a lethal phenotype (YA488, YA491, RA495, HA559, WA569, and M607stop). In addition, two viable mutants (YA565 and MA607) exhibited drastic decreases in k_{cat} values of 17- and 13-fold, respectively. All these residues are located in the helix-bundle domain and altogether contribute to the establishment of an intricate network of interactions that is responsible for the anticodon-loop distortion and binding. The six class Ia synthetases contain a similar antiparallel α-helix bundle appended to the C-terminal end of the Rossmann fold. The structure of this domain varied from a minimalist structure made of four helices (CysRS) (*18*) to larger structures made of five helices connected by variable sized loops (Met-, Leu-, Ile-, Val-, and ArgRS) (*3*, *19*−*22*). So far, three structures of class Ia synthetases in complex with their tRNA have been solved. One is the ternary complex ArgRS:$tRNA^{Arg2}_{ICG}$:arginine studied here (*4*), another one is IleRS:$tRNA^{Ile}$:mupirocin (*23*), and the last one is ValRS:$tRNA^{Val}$:Val-AMS (*22*, *24*). In all three complexes, the tRNA approaches the helix-bundle domain in the same manner as expected from enzymes that derive from a common ancestor. Moreover, one of the key residues for the $tRNA^{Arg}$ recognition (R495 in ArgRS) is also present in IleRS (R653) (*23*) and in ValRS (R587) (*24*) (Figure 2). As the structure of the anticodon loop is different for those three systems, the stabilization of the local tRNA conformations by this conserved arginine residue is idiosyncratic to each of the three aminoacyl-tRNA synthetases. Other class Ia synthetases also share an arginine residue at this position, but structural data of complexes with tRNAs are yet not available (MetRS, CysRS, and LeuRS). However, it was shown that the R residue found at this position in *E. coli* MetRS (R395) plays a determinant role in $tRNA^{Met}$ binding (*25*, *26*). The same was observed in yeast MetRS (*27*). Three other lethal mutations isolated in yeast ArgRS have functional counterparts in MetRS, like residues N391, D449, and W461 that correspond to ArgRS residues Y491, H559, and W569, respectively. In MetRS, it has been shown that these residues are essential for $tRNA^{Met}_{CAU}$ binding and for the discrimination of noncognate tRNAs (*28*−*32*).

Misarginylation of $tRNA^{Asp}$ Is Improved by Mutations in the Anticodon Binding Site. It has been early described that yeast ArgRS misacylates $tRNA^{Asp}$ with arginine in a tRNA-dependent way (*9*). It was proposed that this spontaneous misacylation resulted from an imperfect tRNA recognition that allowed the noncognate $tRNA^{Asp}$ acceptor end to reach the active site pocket in a reactive conformation. Nevertheless, this misacylation only reached 1/2750 of the charging rate of $tRNA^{Arg}$, a value that was significantly enhanced using unmodified synthetic transcripts that relaxed the tRNA structure (*33*, *34*) or by mutating the ACBS of ArgRS (*5*). Therefore, all the factors that improve the fit of the noncognate $tRNA^{Asp}$ increase the misacylation ratio; thus, the misacylation assay can be used as a tool to verify the integrity of the tRNA binding site and the stringency of the tRNA recognition. Among the 14 mutations tested, two mutants, YA491 and RA495, exhibited an increase of the misacylation ratio of $tRNA^{Asp}$ that reached 1/280 and 1/340 of the $tRNA^{Arg}$ charging ratio, respectively. These results suggest that in addition to the binding of the nucleotides Gua36, Ade37, Ade38, and Cyt39, Y491 and R495 act negatively on the noncognate tRNAs such as $tRNA^{Asp}$ and can be considered as antideterminants for the $tRNA^{Asp}$ recognition.

Synergistic Effects on tRNA Aminoacylation and ATP Binding. The kinetic analyses performed on ArgRS variants show that ATP binding is influenced by the lethal mutations that also drastically reduce the tRNA aminoacylation rate. This covariation suggests the presence of a probable link between the tRNA and the ATP binding sites. However, most of the mutations are located in the ACBS domain, more than 30 Å away from the presumed ATP binding site of ArgRS. This would mean that distant effects govern ATP binding and that an accurate binding of the tRNA is a prerequisite for correct binding of ATP, as suggested before (*4*). Indeed, comparison of the tRNA-free ArgRS and ternary ArgRS:$tRNA^{Arg}$:arginine complex reveals that $tRNA^{Arg}$ and arginine binding induce conformational changes that result in a

catalytically competent conformation of ArgRS (*4*). Communication between the ACBS and the catalytic domain of yeast ArgRS has been shown to be mediated through conformational changes of two long helices (H15 and H17) of the helix-bundle domain. Those two helices may serve as a structural path of communication that links the ACBS and HIGH and KMSKS sequences. The function of this path would be to inform the active site of the tRNA binding; consequently, the productive conformation of the catalytic platform will be created. Extensive works on GlnRS and GluRS have also shown that the cognate tRNA has to be considered as an obligate macromolecular cofactor in the first step of the aminoacylation reaction and is therefore required to build up a catalytically competent conformation of the active site of the enzyme. In *E. coli* GlnRS, a structural linkage (a long two-stranded β-ribbon) that may transmit a signal from the ACBS to the active site domain, in the presence of the cognate $tRNA^{Gln}$, has been proposed a long time ago (*35*). The structure of the free GlnRS has now shown that binding of the substrates is coupled to active site assembly and that neither the ATP nor the glutamine binding sites are fully formed in the unliganded GlnRS (*36*). Four new crystal structures of GluRS from *T. thermophilus* have also shown recently that GluRS possesses two modes for ATP binding, a nonproductive and a productive binding mode that can be switched in a tRNA dependent manner (*37*). However, in this case, no structural linkage between the ACBS and the catalytic site has been visualized. The damages on the ATP binding observed in this study confirm the functional role of these movements that link the ACBS and the ATP binding site and suggest that the interdomain communication plays a major role in active site activation of ArgRS. A similar model was suggested for Chinese hamster ovary ArgRS (*38*).

tRNA Aminoacylation Can Be Improved by High Magnesium Concentrations. Aminoacyl-tRNA synthetases display a typical activity curve as a function of the Mg^{2+} concentration, starting by an increase and reaching an optimum at a ratio of Mg^{2+}/ATP close to one for the class I enzymes and three or more for the class II enzymes (*39*, *40*). Up to these values, both activities (amino acid activation and tRNA charging) decrease with the excess of Mg^{2+}. Magnesium ions are cofactors of ATP (one ion for class I enzymes and three for class II enzymes), and in addition, they stabilize the tRNA structure. In the case of native yeast ArgRS, a singularly narrow curve of activity versus Mg^{2+} concentration is observed that renders the activity very sensitive to the Mg^{2+} concentration (*41*). We confirm in our work that a Mg^{2+}/ATP ratio of 0.7:1 is optimal for the wild type enzyme, whereas for the variants of the ACBS, the optimal Mg^{2+}/ATP ratio reaches up to three (Figure 3 and Table 2). With $tRNA^{Arg2}_{ICG}$, this phenomenon was observed for three mutants (RA495, YA565, and WA569), whereas for $tRNA^{Arg3}_{UCU}$, it was observed for all eight mutants of the ACBS. The fact that the lethal mutants were unable to grow suggests that the poor magnesium concentration found in the cell (about 0.1−1 mM) is inadequate to saturate the magnesium binding sites of the mutated enzymes. As the Mg^{2+} mediated reactivation is exclusively observed for variants of the ACBS, it is likely that the extra Mg^{2+} ions bind at the level of the anticodon loop and stabilize a more reactive conformation of the tRNA-enzyme complex. A similar Mg^{2+} dependence was observed with tRNA transcripts from phage T5. It was shown that mutants of the anticodon triplet are more efficiently charged at high Mg^{2+} concentration in contrast to native tRNA and mutants of the Dhu-loop (*42*). These results all together show that increasing the divalent ion concentration can expand the plasticity of the tRNA anticodon loop, and as a result, stabilize the mutated tRNA-enzyme complexes.

Careful examination of the crystallographic structure of the native complex ArgRS:$tRNA^{Arg}_{ICG}$:arginine at 2.2 Å resolution reveals a striking absence of a coordinated divalent ion (*4*). These experimental evidences suggest two possibilities: either the formation of the ArgRS:$tRNA^{Arg}$ complex occurs without Mg^{2+} or the divalent ions are released after complex formation and can no more be detected. Although the hypothesis that no divalent ions are used must still be confirmed, some functional evidences, like the sharp peak of the optimal Mg^{2+}/ATP ratio, agree well with this assumption. Moreover, early studies highlighted the deleterious effect of high Mg^{2+} concentration for tRNA binding. It was shown that high Mg^{2+} concentrations could decrease the aminoacylation rate by increasing the tRNA affinity and consequently by decreasing the dissociation rate of the enzyme−product (*41*).

Lethal Phenotype of WA569 Can Be Reverted by High Mg^{2+} Concentration. Following the in vitro investigations on the Mg^{2+} effect, we asked whether the same phenomenon of reactivation can be observed in vivo, or in other words, if lethal mutations can be rescued by growth on Mg^{2+} enriched media. In yeast cells, the total cellular concentration of Mg^{2+} is in the millimolar range; the vast majority is bound to negatively bound ligands (particularly phosphate, ATP, RNA, and DNA), leaving only a small fraction in the free ionized form (*43*). Cells of the *S. cerevisiae* tightly control intracellular Mg^{2+} levels, allowing only a 3−4-fold decrease, when the external concentration changes 4 orders of magnitude (from 10 μM to 100 mM) (*44*). A Mg^{2+} transporter has recently been identified in the yeast *S. cerevisiae*. The knockout of its gene *ALR1* showed a 60% reduction of total intracellular Mg^{2+} as compared to the wild type and failed to grow in standard media (*45*). We used the shuffle-colored assay to test the effect of Mg^{2+} concentration on the growth of the six lethal mutants involved in the tRNA anticodon binding (YA488, YA491, RA495, HA559, WA569, and M607stop). In this way, we expected to increase the intracellular Mg^{2+} concentration by increasing the external concentration of divalent ions. Yeast cells were grown in minimal medium supplemented with an increasing concentration of $MgCl_2$ from 1 to 500 mM. A toxic effect was observed for all the strains and controls above 100 mM $MgCl_2$. But surprisingly, we observed that the growth of the inactive mutant WA569 was restored on medium containing from 10 to 100 mM Mg^{2+}. This in vivo restoration effect was correlated with a significant increase of the in vitro activity at high Mg^{2+} concentration. At the usual ratio Mg^{2+}/ATP = 1, the activity of mutant WA569 was only 10 and 2.5% of the wild type charging rates of $tRNA^{Arg2}_{ICG}$ and $tRNA^{Arg3}_{UCU}$, respectively. Both activities were increased up to 50 and 45%, respectively, at the more optimal ratio of 2.5 (Table 2). However, this remarkable result is restricted to WA569. Another mutant, HA559, was not rescued despite the fact that it was reactivated up to 33% at the optimal Mg^{2+}

concentration (Table 2). This suggests that the reversion of the lethal phenotype by an increase of the Mg^{2+} concentration can only benefit mutants that are very close to the threshold of cellular viability. Therefore, we propose that the activity of WA569 is below but probably very close to the limit required for cell growth and that the activity of HA559 and of the other lethal mutants is clearly below this limit. The growth-limiting activity can also be approached by the analysis of the aminoacylation rates of the viable mutants (YA565, Table 2). Compared with WA569, the only significant difference concerns the charging rate of $tRNA^{Arg3}_{UCU}$ that is 3-fold reduced. This suggests that WA569 is lethal because of its deficit in $tRNA^{Arg3}_{UCU}$ charging activity. Altogether, these results would place the minimal activity required for growth between lethal WA569 and viable YA565. They also highlight the complexity of the arginine system where lethality can be induced by effects on only one tRNA isoacceptor.

Concluding Remarks. The ArgRS-$tRNA^{Arg}$ recognition system is exceptional because of the presence of several $tRNA^{Arg}$ isoacceptors. The sequence diversity found in these tRNA molecules implies that the atom groups cannot be used for the recognition as in many tRNA-synthetase systems. In contrast to other systems, no lethal mutation corresponding to direct interactions between side chain atoms of the protein and the base moiety of the nucleotides has been found. Most of the crucial interactions occur between the main chain atoms of one residue and the specific groups of the interacting partner (*4*). Therefore, this enzyme is adapted to the recognition of substrates with different sequences. The conformational changes observed on tRNA binding and the plasticity of the tRNA molecule revealed by Mg^{2+} effects illustrate the high degree of adaptability of the tRNA toward the enzyme. Recent investigations on *E. coli* ArgRS-$tRNA^{Arg}$ recognition brought supplementary data that support these observations (*46*). By mutagenesis and kinetic analysis of $tRNA^{Arg}$, it was shown that the enzyme can recognize the identity elements (usually C35 and G36) shifted to the 5′ side by one residue (becoming C34 and G35) (*46*). Moreover, during the misacylation of $tRNA^{Asp}$ by ArgRS, the same dinucleotide CG of $tRNA^{Asp}$ is recognized by ArgRS but at position 36−37 (*17*), which also suggests a shift by one nucleotide but to the 3′ side. The resolution of the crystallographic structure of ArgRS in complex with other tRNA isoacceptors is requested to give a definitive answer on the capacity of the anticodon binding domain to recognize different tRNA substrates.

ACKNOWLEDGMENT

We want to express our gratitude to Dr. J. Gangloff for constant advice, encouragement, and stimulating discussions. We are indebted to Dr. S. Barends for careful reading of the manuscript and Dr. F. Martin for helpful discussions.

REFERENCES

1. Eriani, G., Delarue, M., Poch, O., Gangloff, J., and Moras, D. (1990) Partition of tRNA synthetases into two classes based on mutually exclusive sets of sequence motifs, *Nature 347*, 203−206.
2. Cusack, S., Berthet-Colominas, C., Härtlein, M., Nassar, N., and Leberman, R. (1990) A second class of synthetase structure revealed by X-ray analysis of *Escherichia coli* seryl-tRNA synthetase, *Nature 347*, 249−255.
3. Cavarelli, J., Delagoutte, B., Eriani, G., Gangloff, J., and Moras, D. (1998) L-Arginine recognition by yeast arginyl-tRNA synthetase, *EMBO J. 17*, 5438−5448.
4. Delagoutte, B., Moras, D., and Cavarelli, J. (2000) tRNA aminoacylation by arginyl-tRNA synthetase: induced conformations during substrates binding, *EMBO J. 19*, 5599−5610.
5. Geslain, R., Martin, F., Delagoutte, B., Cavarelli, J., Gangloff, J., and Eriani, G. (2000) In vivo selection of lethal mutations reveals two functional domains in arginyl-tRNA synthetase, *RNA 6*, 434−448.
6. Kunkel, T. A. (1985) Rapid and efficient site-specific mutagenesis without phenotypic selection, *Proc. Natl. Acad. Sci. U.S.A. 82*, 488−492.
7. Eriani, G., Cavarelli, J., Martin, F., Dirheimer, G., Moras, D., and Gangloff, J. (1993) Role of dimerization in yeast aspartyl-tRNA synthetase and importance of the class II invariant proline, *Proc. Natl. Acad. Sci. U.S.A. 90*, 10816−10820.
8. Varshney, U., Lee, C. P., and RajBhandary, U. L. (1991) Direct analysis of aminoacylation levels of tRNAs in vivo. Application to studying recognition of *E. coli* initiator tRNA mutants by glutaminyl-tRNA synthetase, *J. Biol. Chem. 266*, 24712−24718.
9. Gangloff, J., Ebel, J., and Dirheimer, G. (1973) Isolation of a complex between yeast arginyl-tRNA synthetase and yeast tRNA^{Asp} and mischarging of $tRNA^{Asp}$ with arginine, *J. Intl. Res. Commun. 1*, 8.
10. McClain, W. H., and Foss, K. (1988) Changing the acceptor identity of a transfer RNA by altering nucleotides in a "variable pocket", *Science 241*, 1804−1807.
11. Tamura, K., Himeno, H., Asahara, H., Hasegawa, T., and Shimizu, M. (1992) In vitro study of *E. coli* $tRNA^{Arg}$ and $tRNA^{Lys}$ identity elements, *Nucl. Acids Res. 20*, 2335−2339.
12. Schulman, L. H., and Pelka, H. (1989) The anticodon contains a major element of the identity of arginine transfer RNAs, *Science 246*, 1595−1597.
13. Liu, W., Huang, Y., Eriani, G., Gangloff, J., Wang, E., and Wang, Y. (1999) A single base substitution in the variable pocket of yeast $tRNA^{Arg}$ eliminates species-specific aminoacylation, *Biochim. Biophys. Acta 1473*, 356−362.
14. Geslain, R., Martin, R., Camasses, A., and Eriani, G. (2003) A yeast knockout strain to discriminate between active and inactive tRNA molecules, *Nucl. Acids Res. 31*, 4729−4737.
15. Shimada, A., Nureki, O., Goto, M., Takahashi, S., and Yokoyama, S. (2001) Structural and mutational studies of the recognition of the arginine tRNA-specific major identity element, A20, by arginyl-tRNA synthetase, *Proc. Natl. Acad. Sci. U.S.A. 98*, 13537−13542.
16. Sprinzl, M., Horn, C., Brown, M., Ioudovitch, A., and Steinberg, S. (1998) Compilation of tRNA sequences and sequences of tRNA genes, *Nucl. Acids Res. 26*, 148−153.
17. Sissler, M., Giegé, R., and Florentz, C. (1996) Arginine aminoacylation identity is context-dependent and ensured by alternate recognition sets in the anticodon loop of accepting tRNA transcripts, *EMBO J. 15*, 5069−5076.
18. Newberry, K. J., Hou, Y. M., and Perona, J. J. (2002) Structural origins of amino acid selection without editing by cysteinyl-tRNA synthetase, *EMBO J. 21*, 2778−2787.
19. Mechulam, Y., Schmitt, E., Maveyraud, L., Zelwer, C., Nureki, O., Yokoyama, S., Konno, M., and Blanquet, S. (1999) Crystal structure of *Escherichia coli* methionyl-tRNA synthetase highlights species-specific features, *J. Mol. Biol. 294*, 1287−1297.
20. Cusack, S., Yaremchuk, A., and Tukalo, M. (2000) The 2 Å crystal structure of leucyl-tRNA synthetase and its complex with a leucyl-adenylate analogue, *EMBO J. 19*, 2351−2361.
21. Nureki, O., Vassylyev, D., Tateno, M., Shimada, A., Nakama, T., Fukai, S., Konno, M., Hendrickson, T., Schimmel, P., and Yokoyama, S. (1998) Enzyme structure with two catalytic sites for double-sieve selection of substrate, *Science 280*, 578−582.
22. Fukai, S., Nureki, O., Sekine, S., Shimada, A., Tao, J., Vassylyev, D. G., and Yokoyama, S. (2000) Structural basis for double-sieve discrimination of L-valine from L-isoleucine and L-threonine by the complex of $tRNA^{Val}$ and valyl-tRNA synthetase, *Cell 103*, 793−803.
23. Silvian, L. F., Wang, J., and Steitz, T. A. (1999) Insights into editing from an ile-tRNA synthetase structure with $tRNA^{Ile}$ and mupirocin, *Science 285*, 1074−1077.
24. Fukai, S., Nureki, O., Sekine, S., Shimada, A., Vassylyev, D., and Yokoyama, S. (2003) Mechanism of molecular interactions for $tRNA^{Val}$ recognition by valyl-tRNA synthetase, *RNA 9*, 100−111.

25. Ghosh, G., Kim, H. Y., Demaret, J. P., Brunie, S., and Schulman, L. H. (1991) Arginine-395 is required for efficient in vivo and in vitro aminoacylation of transfer RNAs by *Escherichia coli* methionyl-transfer RNA synthetase, *Biochemistry 30*, 11767−11774.
26. Kim, H. Y., Pelka, H., Brunie, S., and Schulman, L. H. (1993) Two separate peptides in *Escherichia coli* methionyl-tRNA synthetase form the anticodon binding site for methionine, *Biochemistry 32*, 10506−10511.
27. Despons, L., Senger, B., Fasiolo, F., and Walter, P. (1992) Binding of the yeast tRNA(Met) anticodon by the cognate methionyl-tRNA synthetase involves at least two independent peptide regions, *J. Mol. Biol. 225*, 897−907.
28. Kim, S., Ribas de Pouplana, L., and Schimmel, P. (1994) An RNA binding site in a tRNA synthetase with a reduced set of amino acids, *Biochemistry 33*, 11040−11045.
29. Ghosh, G., Pelka, H., and Schulman, L. D. H. (1990) Identification of the anticodon recognition site of *Escherichia coli* methionyl-tRNA synthetases, *Biochemistry 29*, 2220−2225.
30. Schmitt, E., Meinnel, T., Panvert, M., Mechulam, Y., and Blanquet, S. (1993) Two acidic residues of *Escherichia coli* methionyl-tRNA synthetase act as negative discriminants towards the binding of noncognate tRNA anticodons, *J. Mol. Biol. 233*, 615−628.
31. Meinnel, T., Mechulam, Y., LeCorre, D., Panvert, M., Blanquet, S., and Fayat, G. (1991) Selection of suppressor methionyl-tRNA synthetases: mapping the tRNA anticodon binding site, *Proc. Natl. Acad. Sci. U.S.A. 88*, 291−295.
32. Auld, D. S., and Schimmel, P. (1995) Switching recognition of two tRNA synthetases with an amino acid swap in a designed peptide, *Science 267*, 1994−1996.
33. Perret, V., Garcia, A., Grosjean, H., Ebel, J.-P., Florentz, C., and Giegé, R. (1990) Relaxation of transfer RNA specificity by removal of modified nucleotides, *Nature 344*, 787−789.
34. Pütz, J., Florentz, C., Benseler, F., and Giegé, R. (1994) A single methyl group prevents the mischarging of a tRNA, *Nat. Struct. Biol. 1*, 580−582.
35. Rould, M. A., Perona, J. J., and Steitz, T. A. (1991) Structural basis of anticodon loop recognition by glutaminyl-tRNA synthetase, *Nature 352*, 213−218.
36. Sherlin, L., and Perona, J. (2003) tRNA-dependent active site assembly in a class I aminoacyl-tRNA synthetase, *Structure 11*, 591−603.
37. Sekine, S., Nureki, O., Dubois, D., Bernier, S., Chenevert, R., Lapointe, J., Vassylyev, D., and Yokoyama, S. (2003) ATP binding by glutamyl-tRNA synthetase is switched to the productive mode by tRNA binding, *EMBO J. 22*, 676−688.
38. Lazard, M., Agou, F., Kerjan, P., and Mirande, M. (2000) The tRNA-dependent activation of arginine by arginyl-tRNA synthetase requires interdomain communication, *J. Mol. Biol. 302*, 991−1004.
39. Kern, D., and Lapointe, J. (1979) The 20 aminoacyl-tRNA synthetases from *Escherichia coli*. General separation procedure and comparison of the influence of pH and divalent cations on their catalytic activities, *Biochimie 61*, 1257−1272.
40. Airas, R. K. (1996) Differences in the magnesium dependences of the class I and class II aminoacyl-tRNA synthetases from *Escherichia coli*, *Eur. J. Biochem. 240*, 223−231.
41. Gangloff, J., Schutz, A., and Dirheimer, G. (1976) Arginyl-tRNA synthetase from baker's yeast. Purification and some properties, *Eur. J. Biochem. 65*, 177−182.
42. Kholod, N. S., Pan'kova, N. V., Mayorov, S. G., Krutilina, A. I., Shlyapnikov, M. G., Kisselev, L. L., and Ksenzenko, V. N. (1997) Transfer RNA^{Phe} isoacceptors possess nonidentical set of identity elements at high and low Mg^{2+} concentration, *FEBS Lett. 411*, 123−127.
43. Romani, A., and Scarpa, A. (1992) Regulation of cell magnesium, *Arch. Biochem. Biophys. 298*, 1−12.
44. Beeler, T., Bruce, K., and Dunn, T. (1997) Regulation of cellular Mg^{2+} by *Saccharomyces cerevisiae*, *Biochim. Biophys. Acta 1323*, 310−318.
45. Graschopf, A., Stadler, J. A., Hoellerer, M. K., Eder, S., Sieghardt, M., Kohlwein, S. D., and Schweyen, R. J. (2001) The yeast plasma membrane protein Alr1 controls Mg^{2+} homeostasis and is subject to Mg^{2+}-dependent control of its synthesis and degradation, *J. Biol. Chem. 276*, 16216−16222.
46. Kiga, D., Sakamoto, K., Sato, S., Hirao, I., and Yokoyama, S. (2001) Shifted positioning of the anticodon nucleotide residues of amber suppressor tRNA species by *Escherichia coli* arginyl-tRNA synthetase, *Eur. J. Biochem. 268*, 6207−6213.
47. DeLano, W. L. (2002) The PyMOL Molecular Graphics System, http://www.pymol.org.
48. Perona, J. J., Rould, M. A., and Steitz, T. A. (1993) Structural basis for transfer RNA aminoacylation by *Escherichia coli* glutaminyl-tRNA synthetase, *Biochemistry 32*, 8758−8771.

BI035581U